INL/CON-07-12478
PREPRINT

Minor Actinide Transmutation for Low Conversion Ratio Sodium Fast Reactors

Global 2007

Rodolfo Ferrer
Samuel E. Bays
Benoit Forget
Mehdi Asgari

September 2007

The INL is a
U.S. Department of Energy
National Laboratory
operated by
Battelle Energy Alliance

Minor Actinide Transmutation for Low Conversion Ratio Sodium Fast Reactors

Rodolfo Ferrer, Samuel E. Bays, Benoit Forget, Mehdi Asgari

Idaho National Laboratory: P. O. Box 1625, MS 3117, Idaho Falls, ID, 83403, Samuel.Bays@inl.gov

The effects of varying the reprocessing strategy used in the closed cycle of a Sodium Fast Reactor (SNF) prototype are presented in this paper. The isotopic vector from the aqueous separation of transuranic (TRU) elements in Light Water Reactor (LWR) spent nuclear fuel (SNF) is assumed to also vary according to the reprocessing strategy of the closed fuel cycle. The decay heat, gamma energy, and neutron emission of the fuel discharge at equilibrium are found to vary depending on the separation strategy. The SFR core used in this study corresponds to a burner configuration with a conversion ratio of ~0.5 based on the Super-PRISM design. The reprocessing strategies stemming from the choice of either metal or oxide fuel for the SFR are found to have a large impact on the equilibrium discharge decay heat, gamma energy, and neutron emission. Specifically, metal fuel SFR with pyroprocessing of the discharge produces the largest amount of TRU consumption (166 kg per Effective Full Power Year or EFPY), but also the highest decay heat, gamma energy, and neutron emission. On the other hand, an oxide fuel SFR with PUREX reprocessing minimizes the decay heat and related parameters of interest to a minimum, even when compared to thermal Mixed Oxide (MOX) or Inert Matrix Fuel (IMF) on a per mass basis. On an assembly basis, however, the metal SFR discharge has a lower decay heat than an equivalent oxide SFR assembly for similar minor actinide consumptions (~160 kg/EFPY.) Another disadvantage in the oxide PUREX reprocessing scenario is that there is no consumption of americium and curium, since PUREX reprocessing separates these minor actinides (MA) and requires them to be disposed of externally.

I. INTRODUCTION

For the past six decades, the dominant once-through fuel cycle strategy in the United States has resulted in the accumulation of LWR SNF, and thus, the need of a permanent geological repository. The long half-life, radiotoxicity, and decay heat of LWR SNF isotopes dictate the design criteria for the geologic repository's storage capacity. A way to maximize repository utilization is to separate the TRU elements from the spent fuel and fabricate these into fuel for a Sodium Fast Reactor[1]. The key advantage in this scenario is the assumption that the reprocessing of TRU in a SFR, along with a low capture-to-fission cross-section in the neutron flux high-energy spectrum, can effectively minimize the long-term decay heat and toxicity of the waste being sent to the repository[2].

Even in a SFR, however, not all transuranic isotopes can fission with the same efficiency. Higher mass actinides such as curium are produced in a transuranic-burning reactor more readily than past SFR fuel cycles because of the fertile americium concentration in SNF. This has a significant impact on the decay heat during the fuel reprocessing and re-fabrication. Furthermore, the threshold fission for most actinides occurs at very high energies, higher than the average neutron energy in a SFR energy spectrum. Thus, homogeneous recycling results not necessarily in the complete destruction of minor actinides, but in the *stabilization* of the amount of MA in the nuclear enterprise that would otherwise be destined to geologic repository disposal. Whether this is the desired or intended effect of current efforts to close the nuclear fuel cycle in the United States is outside the scope of this paper.

The presence of MA in the closed fuel cycle is determined by the LWR SNF separation strategy and the type of SFR fuel reprocessing used. Furthermore, the choice of reprocessing is dependent on the type of fuel selected for the SFR. The interplay between the choice of separation strategy, reprocessing, and type of fuel used is of central importance from both a repository and fuel handling point of view.

The purpose of this work is to study the effects of using different reprocessing strategies for either metal or oxide fuel with compatible LWR SNF separation strategies (such as UREX+ separations). The SFR prototypes used in this study are SuperPRISM[3] (S-PRISM)-based design variations for which the conversion ratio (CR) has been decreased from breakeven to ~0.5 through fuel pin diameter reduction. Previous studies involving the reduction of the conversion ratio in SFR typically involved pancaking[4,5] (geometric spoiling) or the reduction of the fuel pin diameter[6] (or a combination of both[7].)

The rest of this paper is organized in the following manner: Section II describes the methodology used in the analysis, Section III presents the assumptions made and the reactor models used, and Section IV presents the results from the analyses. Finally, conclusions and recommendations for future work are presented in Section V.

II. METHODOLOGY

The Argonne National Laboratory (ANL) fast reactor codes MC^2-2 (Ref. 8) and REBUS-3 (Ref. 9) were used to generate multi-group fast spectrum cross-sections and to perform fuel cycle calculations. The MC^2-2 code was used to generate 33 energy-group cross section sets for each of the driver fuel enrichment zones, reflectors and shields. Starting with an ultra-fine group ENDF-V/B cross section library, MC^2-2 creates collapsed cross section sets by performing a critical buckling search. While this approach does not account for spatial variations within or between the various core regions, it has been proven to be sufficient for fast reactor scoping calculations. The correct treatment of resolved and unresolved resonance self-shielding at operating temperature is of particular importance in this procedure. These cross section sets are consequently concatenated and used by the fuel cycle code REBUS-3 to perform an equilibrium enrichment search for given constraints (such as burnup limit).

The REBUS-3 nodal diffusion option in hexagonal-z geometry was used to perform the flux calculations. In our fuel cycle model individual fuel assemblies are homogenized into "like neutron spectrum" representative enrichment zones. Therefore, independent batches of fuel are tracked within the external fuel cycle but not explicitly spatially represented in the physics calculation. Furthermore, the constraints in the equilibrium calculations involved a search of the specific fresh fuel charge enrichment given a discharge burnup limit. This was done by first estimating the initial fuel composition by assuming a certain approximate enrichment. The fuel cycle code searches for an enrichment that does not violate the maximum burnup limit for the uncontrolled core (the multiplication factor equal to 1.0 at end-of-life). An automated scripting system is used to re-calculate the cross-sections for each enrichment zone based on that zone's fuel inventory at equilibrium. This ensures that the group constants correspond to the equilibrium case (since the initial cross section set is based only on an estimate of the actual TRU enrichment). Finally, the corrected charge enrichment and equilibrium cycle length is reported. The peak fast flux was used to calculate the peak fast fluence and a limit of 4.0×10^{23} n/cm^2 for HT9 cladding and structure was assumed to be the fluence limit[10-12].

Since REBUS only deals with the closed portion of the fuel cycle, the externally supplied feed is made sufficiently large enough to subsidize the reprocessing with enough heavy metal to constitute the next batch of fresh fuel.

Finally, the SCALE 5.1 code package[13] was used to calculate the decay heat, gamma heat, and neutron emission from the equilibrium discharge reported by REBUS-3. Furthermore, ORIGEN-S[14] was used to perform these calculations and decay the discharge out to 20 years.

III. ASSUMPTIONS AND MODELS

In this section the SFR models and their corresponding external fuel cycle are discussed. It is assumed that it is sufficient for the reactor physics calculations to track isotopes up to Cm-246 in the transmutation chain model. It is important to note, however, that decay heat, gamma energy, and neutron emission calculation will be affected if all the isotopes up to Cf-252 are tracked. The effect of tracking higher mass actinides is the subject of a separate study[15] performed by this group.

III.A. Fast Reactor Models

The strategy followed in the reduction of the conversion ratio of the SFR models from the original S-PRISM designs is to reduce the fuel pin diameter in the fuel assemblies. This results in a reduction of the fuel volume fraction and a subsequent increase in the TRU enrichment. A higher TRU enrichment increases the TRU fission relative to the U-238 capture, thus reduces the conversion ratio. This procedure is similar to that used by previous investigators[6]. The choice of a SFR with CR=0.5 represented a modest compromise between the needs to burn TRU and the material irradiation experience from past test programs[10-12].

The fuel assembly design cold dimensions for the reference SFR (either metal or oxide) are listed in Table I. The fuel pin design and volume fractions are presented in Table II. While the S-PRISM assembly design has 271 pins per assembly, the assembly design for the SFR of CR=0.5 has 324 pins per assembly. The reduced thermal performance of higher TRU enriched fuel pins required a larger number of pins per assembly in order to reduce the average linear power to an acceptable limit. The shrinking of the fuel pin diameter also entails using spacer grids instead of wire wrap in the assembly design.

Table I. SFR Fuel Pin Design

Assembly pitch, cm	16.142
Inter-assembly gap, cm	0.432
Duct outside flat-to-flat, cm	15.710
Duct material	HT9
Duct thickness	0.394
Spacer type	Grid

Table II. SFR Fuel Pin Design

	Oxide	Metallic
Fuel Pins per Assembly	324	324
Pin Data:		
Bond	He	Na
Core Height, cm	137.16	101.06
Plenum Height, cm	170.82	191.14
Pin Diameter, cm	0.658	0.623
Pin-to-Pitch-to-diameter Ratio	1.224	1.293
Volume Fractions, %:		
Fuel	30.22	22.08
Bond	1.56	7.36
Structure	29.22	26.41
Coolant	39.00	44.15

III.A.1. Metal Fuel SFR

The radial layout of the metal core consists of three driver fuel regions; the inner, middle, and outer core. A schematic of this layout is shown below in Figure 1. The inner core consists of four rings containing a total of 42 assemblies. The middle core consists of two rings containing a total of 66 assemblies with a charge TRU enrichment of 1.25 of that of the inner core. Finally, the outer core consists of a single ring containing 36 assemblies with a charge TRU enrichment of 1.50 of that of the inner core. Such an enrichment splitting allows for the flattening of the power distribution. The reflector and shield regions of the core correspond to the last three rings of the core. While the ultimate shutdown and primary control rods are shown in the schematic, these were modeled as fully withdrawn.

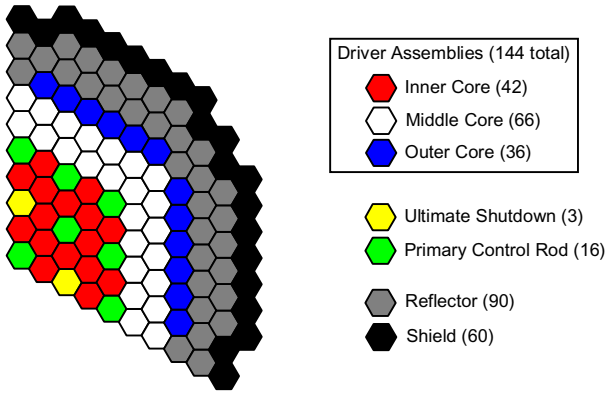

Fig. 1. 1/3 Symmetric radial core layout of metal fuel SFR CR=0.5.

III.A.2. Oxide Fuel SFR

The radial layout of the oxide core, similar to the metal SFR, consists of three driver fuel regions; the inner, middle, and outer core. A schematic of this layout is shown below in Figure 2. The inner core consists of five rings containing a total of 72 assemblies while the middle core consists of one ring containing a total of 36 assemblies with a charge TRU enrichment of 1.25 of that of the inner core. Finally, the outer core consists of a single ring containing 36 assemblies with a charge TRU enrichment of 1.50 of that of the inner core. The reflector, shield, the ultimate shutdown and primary control rods were modeled as fully withdrawn.

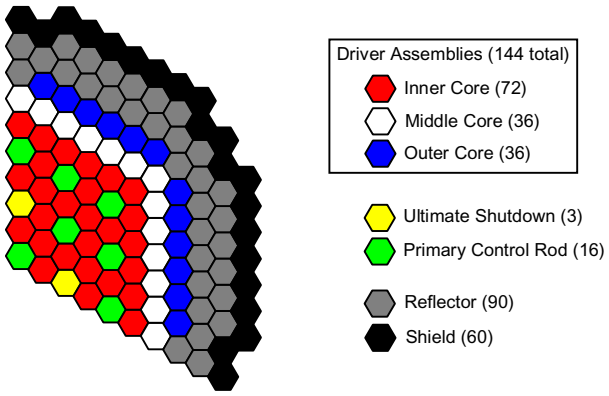

Fig. 2. 1/3 Symmetric radial core layout of oxide fuel SFR CR=0.5.

III.B. External Fuel Cycle Models

In this study, the TRU component of LWR SNF was assumed to be separated through aqueous separation and sent to the fuel fabrication plant to be converted into SFR fuel. Depleted uranium from enrichment plants is assumed to be the only other external feed to provide fuel material to the fuel fabrication plant. The fuel fabrication plant feeds the SFR with the necessary charge isotopic vector. The discharged fuel from the reactor is reprocessed through pyroprocessing (in the case of metal fuel) or aqueous separation (in the case of oxide fuel), and charged back into the SFR. The reduced waste from this fuel cycle is assumed to be sent to interim storage or geologic repository. A schematic of this process is presented below in Figure 3.

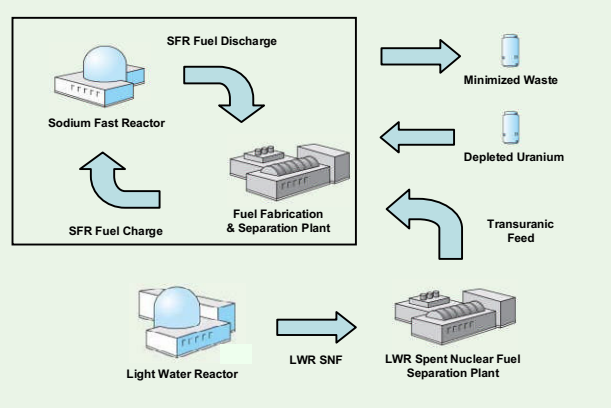

Fig. 3. Reference external fuel cycle for SFR (metal and oxide fuel cases).

The composition of the LWR SNF external feed is presented below in Table III.

Table III. LWR SNF External Feed 50 GWd 5 yr cooled.

TRU Isotopes	w/o
Np-237	4.777
Pu-236	0.000
Pu-238	2.310
Pu-239	47.899
Pu-240	22.510
Pu-241	10.580
Pu-242	6.519
Am-241	3.356
Am-242m	0.006
Am-243	1.475
Cm-242	0.000
Cm-243	0.005
Cm-244	0.515
Cm-245	0.041
Cm-246	0.005

III.B.1. Alternate Metal Fuel SFR External Fuel Cycles

Two alternate external fuel cycles for the metal fuel SFR are analyzed in this study. The first involves the separation of neptunium and plutonium from the LWR SNF (UREX+3) and reprocessing of SFR discharge homogeneously through pyroprocessing. The second alternate external fuel cycle involves the separation of plutonium (PUREX) and reprocessing through the same pyroprocessing technique. In both cases it is assume that americium and curium are disposed of through storage and some specialized target for burning. A schematic of these alternate external cycles is presented in Figure 4.

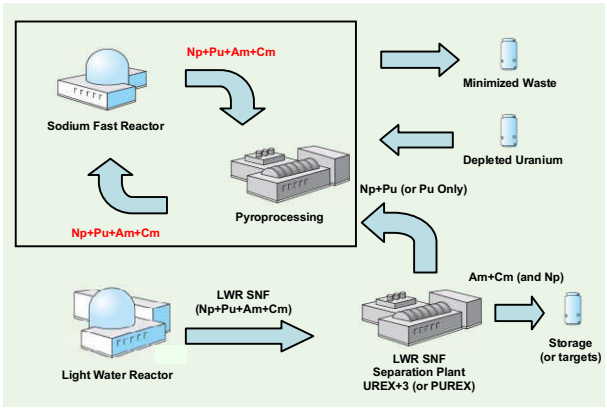

Fig. 4. Simplified conceptual external fuel cycle for SFR.

Due to the nature of reprocessing fuel discharged through pyroprocessing, the entire MA produced in a cycle burn gets charged again into the SFR as part of the fresh fuel. Such feature is highlighted by red letters in the schematic.

III.B.2. Alternate Oxide Fuel SFR External Fuel Cycles

The alternate external fuel cycles for the case of aqueous reprocessing of oxide fuel offers a wider variety of possible groupings of isotopes than in the case of pyroprocessing metal fuel. In the case of oxide fuel, the minor actinides can be isolated from each other in the fuel discharge and disposed of in different ways. This features in unique to the UREX+ aqueous separation process. The case of using UREX+1a for aqueous separation yields a parallel process to that of pyroprocessing metal fuel in which all the transuranic are fabricated into fresh fuel and charged back into the SFR.

In the case of alternate oxide fuel external cycles, the LWR SNF is separated through UREX+3 or PUREX (identical to the metal fuel SFR). The difference between these two cases is in the reprocessing. While in the case of metal fuel all the TRU is charged back into the reactor, in the case of oxide it is possible to partition the americium and curium (and neptunium) from the discharge. Thus, at equilibrium, the oxide SFR is producing americium and curium and assuming that it being disposed by repository means or some potential target-burning strategies. A schematic of these alternate cycles is presented below in Figure 5 and highlighted in red letters.

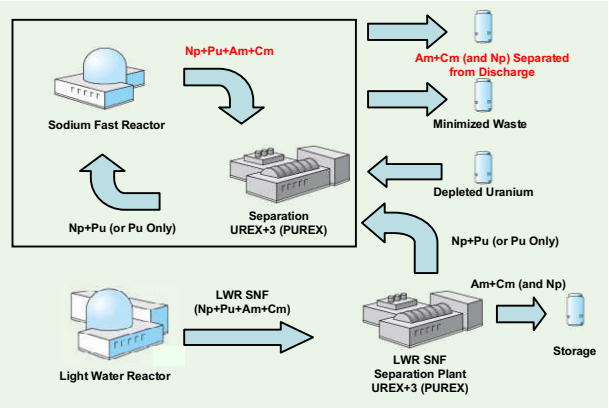

Fig. 5. Simplified conceptual external fuel cycle for SFR.

IV. ANALYSIS RESULTS

The proposed alternate external fuel cycles described in the previous section produced two sets of results; one for the metal fuel and another for the oxide fuel SFR. Each of these cases two SFR designs produced three possible scenarios; one in which PUREX is used on the LWR SNF, another in which UREX+3 is used, and a reference in which a common strategy of leaving all MA in the reprocessing is applied.

IV.A. Fuel Cycle Results

IV.A.1. Metal SFR Results

As expected, no major variations were found when the external fuel cycle strategy was perturbed. Starting with the reference case (where all TRU is reprocessed), the charge enrichment for each zone decreases as the TRU is removed. The presence of more plutonium in place of TRU causes an increase in reactivity and thus a smaller TRU enrichment to meet the cycle length. The rest of the parameters are summarized in Table IV.

Table IV. Fuel Cycle Parameters for the Metal Fuel SFR with varying external feeds (and pyroprocessing).

		Metal fuel SFR		
		Pu	Np+Pu	Np+Pu+Am+Cm
Conversion Ratio		0.58	0.56	0.56
Charge Enrichment, TRU/HM (v/f)	IC	25.7%	26.0%	26.6%
	MC	32.2%	32.4%	33.2%
	OC	38.6%	38.9%	39.9%
Fuel residence time, cycles	IC	6	6	6
	MC	6	6	6
	OC	7	7	7
Burnup (MWd/kg)	Ave. Driver	129	129.8	129.6
HM loading, kg		9,474	9,478	9,422
TRU loading, kg		2,925	2,952	3,005
Fissile Pu loading, kg		1,362	1,348	1,324
Cycle length, EFPD		216	216	216
TRU Consumption Rate, kg/EFPY		160	162	166
TRU Charge, kg/EFPY		862	870	886
HM Charge, kg/EFPY		2743	2744	2729

The rate of consumption (kg per EFPY) for americium and curium are shown in Figure 6. As the figure shows, the consumption in the case where all TRU from LWR SNF is introduced as makeup feed consumes Am-241 at a rate close to 7.89 kg/EFPY. It also consumes Am-243 coming from the makeup feed at a rate of 2.49 kg/EFPY. The capture of a neutron by Am-241 leads 90% of the time to Am-242, which has a 16 hour half-life and subsequently decays into Cm-242 through beta decay (this accounts for the production of Cm-242 shown in Figure 6.) This also accounts for the all the consumption of Am-241, even when not introduced from makeup feed. It's presence is due to beta decay of Pu-241, which has a 14.4 year half-life.

The other important trend to note is the production of Cm-244 in the case of PUREX and UREX+3 LWR SNF separations. The production of this Cm-244 comes from the Am-243 capturing a neutron, becoming Am-244 (which had a 10.1 hour half-life), and decaying into Cm-244. Thus the presence of Am-241 and Am-243 built up from decay and capture eventually lead to their transmutation into Cm-242 and Cm-244, respectively.

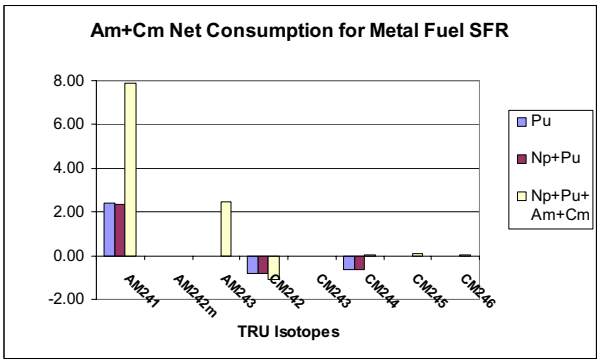

Fig. 6. Americium and Curium Consumption in kg/EFPY for metal fuel SFR (negative consumption is to be understood as production of isotope.)

IV.A.2. Oxide SFR Results

While the external fuel cycle for the oxide SFR is different from the metal SFR (reprocessing is performed via aqueous separation instead of pyroprocessing), the conclusion that the subtraction of MA does not cause any major variations in the fuel cycle parameters still remains true. The enrichment required to meet the cycle length decreases as MA is taken out of the external fuel cycle, as expected from the previous case. The larger change in percent TRU enrichment between metal and oxide is due to the fact that the oxide is physically a larger core. A summary of all the other fuel cycle parameters is shown in Table V.

Table V. Fuel Cycle Parameters for the Oxide Fuel SFR with varying external feeds and reprocessing (PUREX, UREX+3, and UREX+1a).

		Oxide fuel SFR		
		Pu	Np+Pu	Np+Pu+Am+Cm
Conversion Ratio		0.59	0.59	0.57
Charge Enrichment, TRU/HM (v/f)	IC	30.3%	30.6%	31.9%
	MC	37.8%	38.3%	39.9%
	OC	45.4%	46.0%	47.9%
Fuel residence time, cycles	IC	6	6	6
	MC	6	6	6
	OC	7	7	7
Burnup (MWd/kg)	Ave. Driver	158.6	158.6	158.5
HM loading, kg		11,473	11,475	11,479
TRU loading, kg		4,056	4,106	4,286
Fissile Pu loading, kg		1,934	1,914	1,792
Cycle length, EFPD		326	326	326
TRU Consumption Rate, kg/EFPY		152	156	163
TRU Charge, kg/EFPY		793	803	837
HM Charge, kg/EFPY		2231	2231	2231

In the case of the oxide SFR, the consumption rates are different from the case of the metal SFR. The first obvious difference is the production of americium and curium for the cases in which PUREX and UREX+3 are used for both LWR SNF TRU separation and reprocessing of oxide fuel discharge. In the case of UREX+1a for both the LWR SNF and the reprocessing, the same trend as the metal fuel case is encountered.

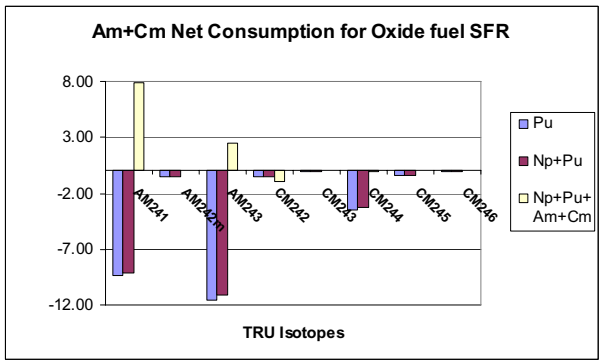

Fig. 7. Americium and Curium Consumption in kg/EFPY for oxide fuel SFR (negative consumption is to be understood as production of isotope.)

It is of interest to note one last point regarding the differences in the metal and oxide fuel cycle. In the case of UREX+1a reprocessing of the oxide fuel, the same pattern in consumption/production can be seen as in the metallic pyroprocessing. Mainly that Am-241 and Am-243 are transmuted into Cm-242 and Cm-244, respectively, from the capture of a neutron by the nuclei. Thus it is worthwhile to note that in a SFR burner scenario (CR < 1), the fission of MA is accompanied by the capture and production of higher mass actinides. This perhaps raises the question of how will geologic repository be affected if Am-241 and Am-243 are, in a sense, interchanged, with Cm-242 and Cm-244. Tabulated results are presented in Table VI below.

Table VII. Tabulated Results of Consumption Rate (kg/EFPY) for metal and oxide SFR.

	Metallic-fueled ABR			Oxide-fueled ABR		
	Pu	Np+Pu	Np+Pu+Am+Cm	Pu	Np+Pu	Np+Pu+Am+Cm
NP237	0.03	8.13	7.90	-0.78	9.16	7.73
PU236	0.00	0.00	0.00	0.00	0.00	0.00
PU238	4.77	4.52	4.68	4.99	4.70	4.46
PU239	85.09	81.94	79.44	96.36	92.39	77.77
PU240	40.77	39.26	38.26	45.60	43.72	37.53
PU241	16.53	15.89	15.37	18.81	17.99	14.92
PU242	11.73	11.29	10.95	13.28	12.73	10.72
AM241	2.39	2.33	7.89	-9.32	-9.12	7.86
AM242m	-0.01	-0.01	0.00	-0.48	-0.46	0.00
AM243	0.00	0.00	2.49	-11.55	-11.09	2.43
CM242	-0.82	-0.80	-1.12	-0.52	-0.50	-0.97
CM243	0.00	0.00	0.01	-0.03	-0.03	0.00
CM244	-0.65	-0.63	0.06	-3.47	-3.30	-0.02
CM245	0.00	0.00	0.07	-0.42	-0.39	0.07
CM246	0.00	0.00	0.01	-0.02	-0.02	0.01
Total	159.83	161.93	166.01	152.45	155.78	162.52

IV.B. Reactor Discharge Calculations

The equilibrium discharge mass data for all the alternate external fuel cycle scenarios was processed through ORGEN-S in order to calculate decay heat, gamma energy, and neutron emission. In the case of the decay heat it is very important to judge the data in a per mass and per assembly basis.

IV.B.1. Decay Heat Calculations

The decay heat calculation of the reactor discharge for the oxide and metal fuel is compared to thermal IMF and MOX recycling in Figure 8 below. In the case of a metal SFR with pyroprocessing, the discharge decay heat remains somewhat invariant to the actinide grouping for the LWR SNF TRU coming from the aqueous separation plant. There is only a slight increase when the LWR SNF americium and curium are included as makeup feed along with the rest of the TRU. The reason for this invariant feature is that Am-241 accumulates in the fuel cycle by way of beta decay from Pu-241. Because the pryroprocessor does not discriminate americium from the rest of the TRU, it includes Am-241 in the next fresh fuel batch. Therefore, Am-241 and the higher mass actinides such as Cm-244 that result from its transmutation, build to an equilibrium concentration after many reactor passes,

In the case of the oxide SFR fuel cycle the decay heat of the discharge increases by almost a magnitude by going from PUREX to UREX+1a. The reason for this increase is that, unlike in the case of pyroprocessing, the PUREX process separates the americium and curium from the discharge and only leaves the plutonium available to the next fuel batch. Similar effects can be seen in thermal MOX and IMF. In the case where all TRU is reprocessed together, thermal IMF has the highest discharge decay heat due to its high content of americium and curium.

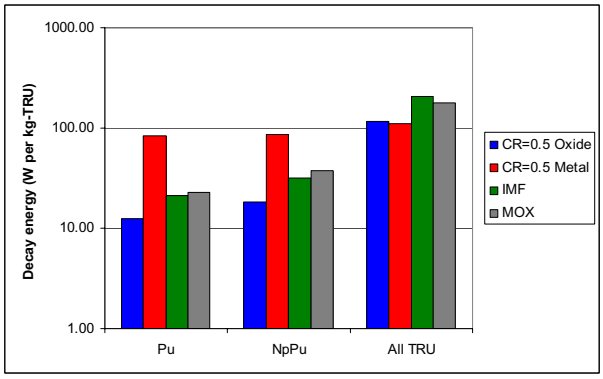

Fig. 8. Decay Heat (logarithmic scale) of Discharge Fuel for SFR (metal and oxide) and thermal recycling (MOX and IMF) on a per mass basis.

An equally important measure of the decay heat is the decay heat per assembly. In fact, from a fuel handling perspective, the decay heat per assembly is a better feature than decay heat per mass, since in reality one would have to deal with physical reactor assemblies being moved. Such data has been tabulated in Table VII below. From this table it is evident that, while oxide has a lower decay heat on a per mass basis, on a per assembly basis it is higher than metal fuels. Such results are expected, since physically the oxide assemblies are simply larger than the metal assemblies since the core is ~37% taller.

Table VII. Decay Heat Results for Span of 20 years for metal and oxide SFR.

		Maximum Decay Heat (watts) per Assembly (Over Span of 20 Years)						
		0	0.01	1	3	5	15	20
Homogeneous Oxide ABR	Pu	9,343	6,690	857	297	187	137	131
	Np+Pu	10,480	7,500	964	350	228	168	159
	All TRU	11,780	8,635	1,405	645	491	346	306
Homogeneous Metal ABR	Pu	8,140	5,839	873	366	266	186	166
	Np+Pu	8,133	5,839	880	378	279	199	179
	All TRU	8,425	6,096	985	437	332	238	213

IV.B.2. Gamma Energy Calculations

The gamma energy produced by discharged fuel is compared in Figure 9 for all cases. The trends for the oxide and metal SFR remain similar to the case of the discharge decay heat calculation. In the case of the oxide SFR, the gamma energy increases the most when the americium and curium are added into the reprocessing. Due to the continual reprocessing of all TRU, the metal SFR discharge remains somewhat invariant with regards to its gamma energy emission.

Similarly to the decay heat calculation, the gamma energy for thermal MOX and IMF on a per mass basis is larger than the SFR discharge for the case where all the TRU are used to make the fuel.

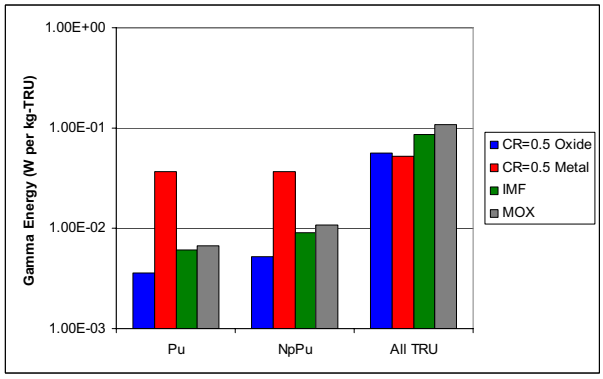

Fig. 9. . Gamma Energy (logarithmic scale) of Discharge Fuel for SFR (metal and oxide) and thermal recycling (MOX and IMF) on a per mass basis.

IV.B.3. Neutron Emission Calculations

Finally, the neutron emission is presented for all four cases in Figure 10 below. Once again, a similar trend is observed as in the decay heat and gamma energy emission calculation. The oxide SFR discharge neutron emission increases in the case where the americium and curium are included in the fuel.

In the case of thermal MOX and IMF, the neutron emission is about two orders of magnitude higher than the metal or oxide SFR on a per mass basis. This is due to the thermal transmutation of americium into high mass actinides.

Finally, it is important to note that these calculations do not track the higher mass actinides (Cm-247 and above.) The inclusion of these isotopes, specially the californium, will increase the neutron emission. While only small amounts of higher mass actinides are produced and destroyed in the SFR fuel cycle, small quantities can have large effects of other parameters, such as neutron emission, for example.

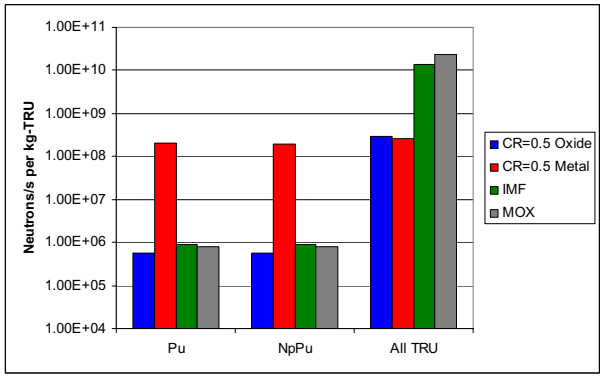

Fig. 10. Neutron emission (logarithmic scale) of Discharge Fuel for SFR (metal and oxide) and thermal recycling (MOX and IMF) on a per mass basis.

V. CONCLUSIONS

The purpose of this study is to understand the effect that different separations and reprocessing methods can have on discharge parameters given either a metal or oxide SFR fuel cycle. It was found that different separations and reprocessing strategies does not significantly alter the fuel cycle characteristics within a given reactor type (metal, oxide). The underlying assumption is that these variations are small and that the given reactor design has a CR of 0.5. The reprocessing strategy does have a significant affect on decay heat, gamma and neutron emission for contrasting fast reactor and LWR fuel types. In case of potential fertile free cores, other parameters of great importance must be addressed (such as Doppler and sodium void coefficients).

An important aspect of the reprocessing of metal fuel through pyroprocessing is the reintroduction of americium and curium. The decay heat, gamma heating, and neutron emission for all separation strategies (PUREX, UREX+3, and UREX+1a) remain close to one another. Thus, no significant reduction in the decay heat, gamma energy, or neutron emission is found by excluding the americium and curium (and neptunium) from entering the fuel cycle.

In the case of oxide SFR discharge, the decay heat, gamma energy, and neutron emission were found to have the greatest decrease when americium and curium are separated both from LWR SNF and in the reprocessing and assumed to be disposed of somewhere else. The drawback here is the accumulation of americium and curium at a rate of ~25 kg/EFPY.

A potential use of this accumulated americium and curium in oxide SFR is the reintroduced into the reactor for transmutation in the form of targets. Current efforts involve the investigation of targets in oxide and metallic-fueled ABR as once-through or continual reprocessing.

ACKNOWLEDGMENTS

We would like to acknowledge Steve Piet and Massimo Salvatores for their guidance and mentoring in the areas of systems analysis and fast reactor physics.

This work was supported by the United States Department of Energy.

REFERENCES

1. D. C. WADE, R. N. HILL, "The Design Rationale of the IFR," *Progress in Nuclear Energy*, **31**, 1-2, 13-42 (1997).
2. R. A. WIGELAND and T. H. BAUER, "Repository Benefits of AFCI Options," Argonne National Laboratory, ANL-AFCI-129, September (2004).
3. A. E. DUBBERLEY, K. YOSHIDA, C. E. BOARMAN, and T. WU, "SuperPRISM Oxide and Metal Fuel Core Designs," *Proc. of ICONE 8, 8th International Conference on Nuclear Engineering* (2000).
4. R. N. HILL, D. C. WADE, E. K. FUJITA, and H. KHALIL, "Physics Studies of Higher Actinide Consumption in an LMR," *Proc. Int. Conf. on the Physics of Reactors*, Marseille, France, p.I-83, April 23-27 (1990).
5. R. N. HILL, D. C. WADE, J. R. LIAW, and E. K. FUJITA, "Physics Studies of Weapons Plutonium Disposition in the Integral Fast Reactor Closed Fuel Cycle," *Nuclear Science and Engineering,* **121**, 17 (1995).
6. E. A. HOFFMAN, W. S. YANG, and R. N. HILL, "Preliminary Core Design Studies for the Advanced Burner Reactor over a Wide Range of Conversion Ratios," Argonne National Laboratory, ANL-AFCI-177 (2006).
7. M. A. SMITH, E. E. MORRIS, R. N. HILL, "Physics and Safety Studies of Low Conversion Ratio Sodium Cooled Fast Reactors", *Global 2003*, New Orleans, Louisiana, United States, pp. 423-433, November 16-20 (2003).
8. H. HENRYSON II, B. J. TOPPEL, and C. G. STENBERG, "MC^2-2: A Code to Calculate Fast Neutron Spectra and Multi-Group Cross-Sections." ANL-8144, Argonne National Laboratory (1976).
9. B. J. Toppel, "A User's Guide to the REBUS-3 Fuel Cycle Analysis Capability," ANL-83-2, Argonne National Laboratory (1983).
10. C. E. LAHM, J. F. KOENIG, R. G. PAHL, D. L. PORTER, and D. C. CRAWFORD, "Experience with Advanced Driver Fuels in EBR-II," *Journal of Nuclear Materials*, **204**, 119 (1993).
11. R. B. BAKER, F. E. BARD, R. D. LEGGETT, and A. L. PINTER, "Status of Fuel, Blanket, and Absorber Testing in the Fast Flux Test Facility," *Journal of Nuclear Materials*, **204**, 109 (1993).
12. A. L. PINTER and R. B. BAKER, "Metal Fuel Test Program in the FFTF," *Journal of Nuclear Materials*, **204**, 124 (1993).
13. *SCALE: A Modular Code System for Performing Standardized Computer Analyses for Licensing Evaluation*, ORNL/TM-2005/39, Version 5.1, Vols. I-III, November 2006. Available from Radiation Safety Information Computational Center at Oak Ridge National Laboratory as CCC-732.
14. *ORIGEN-S: Scale System Module to Calculate Fuel Depletion, Actinide Transmutation, Fission Product Buildup and Decay, and Associated Radiation Source Terms*, ORNL/TM-2005/39, Version 5.1, Vol. II, Book 1, Sect. F7, November 2006. Available from Radiation Safety Information Computational Center at Oak Ridge National Laboratory as CCC-732.